EurJIC
European Journal of Inorganic Chemistry

Research Article
doi.org/10.1002/ejic.202200221

Chemistry Europe
European Chemical Societies Publishing

www.eurjic.org

# A Bispidine Based $Cu^{II}/Zn^{II}$ Heterobimetallic Coordination Polymer

Martina Lippi,[a] Hubert Wadepohl,[b] Peter Comba,[b, c] and Massimo Cametti*[a]

The metalloligand approach was used to obtain a novel $Cu^{II}/Zn^{II}$ heterobimetallic coordination polymer (CP) **1**, based on the carefully designed bispidine ligand **L4**. CP **1**, characterized by single crystal (SC-) and powder X-ray diffraction methods (P-XRD), is constituted by repeating large 32-membered macrocycles forming ribbon-like linear arrays and it features a $Cu^{II}$-coordination site occupied by a markedly labile MeCN. We also describe the synthesis and characterization of intermediate metalloligands (with $Cu^{II}$, $Fe^{III}$, $Mn^{II}$, and $Pd^{II}$, the latter three obtained as SCs and characterized accordingly) and provide a view of potential intermediate species along the route from metalloligands to heterometallic CPs.

## Introduction

Research on coordination polymers (CPs) has witnessed an ever increasing multidisciplinary interest in recent years due to their potential applications in many different areas, such as adsorption, separation and storage of chemicals, sensing, catalysis and also in electronics.[1] CPs are constituted of organic ligands and metal ions or clusters, which can combine into 1D, 2D or 3D architectures,[1,2] following the well-established rulebook of self-assembly based on coordination and supramolecular chemistry.[3] A large variety of different CPs have been reported in the literature,[1,2,4] and many more will come given the virtually infinite collection of suitable ligands, increasingly structurally complex,[5] which can be envisaged and reacted with partnering metal ions or clusters. One particular class of CPs is that represented by heterometallic CPs which present two or more metal ions of different nature.[6] The advantage of such systems over homo-metallic ones can be twofold. First of all, they can give access to even more diversified topologies and architectures by exploitation of two (or more) different metal-ligand interaction geometries. Metal ions in all CP systems have a structural role (*i.e.*, they contribute to sustain the framework and to define the final CP architecture) but they can also have a functional use. That is the case in frameworks with unsaturated metal sites, which can be available for a specific function, for example, in adsorption or catalysis.[7] In heterometallic systems, it is therefore possible to separate the structural role from the functional one by making use of different metal sites, each specialized for a specific role and selected accordingly. Also, electronic interaction between two (or more) different metal centers could lead to novel magnetic properties and spintronic applications.[8]

A common strategy for constructing heterometallic CPs is based on a two-step process involving the formation, as key intermediate, of a metalloligand,[9] *i.e.*, a metal complex capable of acting as a ligand for further interactions with a second metal ion extending the framework; however, other options are also possible.[10]

Recently, we have developed 1D CPs based with bispidine ligands. This class of ligands is especially interesting due to the presence of a rigid bicyclic core, which can be functionalized quite easily by introducing different metal donor sites.[11] Plenty of bispidine metal complexes have been reported. Tetra- and penta-dentate ligands such as **L1** and **L2** are most common (Scheme 1a),[11,12] but ligands with higher denticity have also been conceived (up to being nonadentate towards $Ln^{III}$ ions).[13] In terms of CPs formation, the use of divergent pyridine units, such as in ligand **L3** (Scheme 1b) grants the construction of linear 1D ribbon-like arrays when reacting with $Mn^{II}$ ions. These 1D CPs showed marked dynamic behavior upon adsorption and exchange of volatile solvent guests.[14] One limit of the design of **L3** is related to the aromatic CHs of the para-substituted pyridine rings (indicated by the arrow in Scheme 1b), which hinder metal coordination to the aliphatic Ns, whose functional role remains thus unused.

Here, we report on the first heterometallic bispidine-based CP built with the heptadentate ligand **L4** (Scheme 1c). This ligand was designed having in mind **L2** (Scheme 1a), and other structurally related ligands, whose metal complexes, in particular with $Fe^{II}$ and $Cu^{II}$, demonstrated to be capable of acting as catalyst in several different types of reactions.[15] Stable bispidine metal complexes were also studied extensively in optical and radio-imaging.[12b,16] Thus, **L4** is composed of a classic bispidine core, which is endowed with a pentadentate

[a] *Dr. M. Lippi, Prof. Dr. M. Cametti*
*Department of Chemistry, Materials and Chemical Engineering,*
*Politecnico di Milano*
*Via Luigi Mancinelli 7, 20131, Milano, Italy*
*E-mail: massimo.cametti@polimi.it*
[b] *Prof. Dr. H. Wadepohl, Prof. Dr. P. Comba*
*Anorganisch-Chemisches Institut,*
*Heidelberg University*
*Im Neuenheimer Feld 270, 69120 Heidelberg, Germany*
[c] *Prof. Dr. P. Comba*
*Interdisciplinary Center for Scientific Computing,*
*Heidelberg University*
*69120 Heidelberg, Germany*

*Supporting information for this article is available on the WWW under https://doi.org/10.1002/ejic.202200221*

Research Article
doi.org/10.1002/ejic.202200221



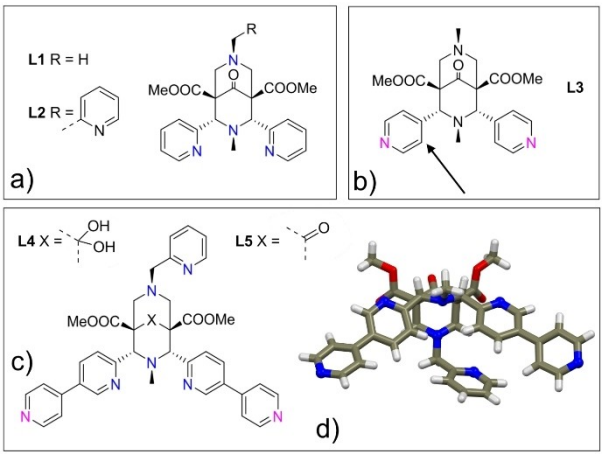


**Scheme 1.** a) Chemical formulae of classic bispidine based tetra- and pentadentate ligands **L1** and **L2**; b) chemical formula of ligand **L3** previously studied and capable to form coordination polymers;[14] c) chemical formulae of ligands **L4** and **L5** used in this work d); view of the structure of **L5** obtained by SC-XRD analysis (Supporting Information). Color code: C = dark grey; H = white; N = blue; O = red.

inner site, but it is also decorated with two adjunct divergent pyridine units. These latter groups serve as donor sites for allowing coordinative polymerization. By implementing a classic two-step synthetic approach, we first obtained a series of molecular complexes with $Mn^{II}$, $Fe^{III}$, $Cu^{II}$ and $Pd^{II}$. In the case of $Mn^{II}$, $Fe^{III}$ and $Pd^{II}$, SCs (for complexes of composition {[$Mn^{II}$-(**L4**)(Cl)]Cl · 1,2DCB}, {[$Fe^{III}$(**L4**)(Cl)]$Cl_2$/[$Fe^{III}$(**L4**)(Cl)]O-$FeCl_3$}, and {[$Pd^{II}$(**L4**)(Cl)]Cl·$CHCl_3$·$H_2O$}) were characterized by SC-XRD (1,2DCB = 1,2-dichlorobenzene). Finally, by reacting complex {[$Cu^{II}$(**L4**)(OTf)]OTf} with $Zn^{II}$ ions, we obtained the $Cu^{II}$/$Zn^{II}$ heterometallic CP **1**, of composition {[(**L4**-$Cu^{II}$-MeCN]$_2$$(OTf)_4$-[$Zn^{II}$$(H_2O)_2$]$(NO_3)_2$$(MeCN)_2$$(H_2O)$}$_n$ (OTf = triflate ion). We here present a detailed description of its structure and, more briefly, of a couple of heterometallic intermediate species isolated along the path undertaken to obtain it, but only partially characterized. CP **1** has all the characteristics to be promising in transferring $Cu^{II}$-bispidine catalytic activity (and eventually that of $Fe^{II}$-based catalysts) from homogeneous to heterogenous conditions, with all the related benefits.[17]

## Results and Discussion

Ligand **L5** is synthesized in a two-step process in 72% yield (see SI), and its X-ray determined structure is shown in Scheme 1d (Figure S9 in SI). Metal complexes (metalloligands) were obtained either by reacting **L5** with the metal salts under refluxing conditions in MeOH, followed by recrystallization of the precipitate formed upon cooling (SI), or by slow crystallization by using a three-layer crystallization method.[18] In all cases, upon complexation at its inner site, the ligand undergoes addition of water to the carbonyl group, and all complexes have been obtained with the ligand in its hydrated form (as in **L4**) (SI).[19]

### X-ray structures of $Mn^{II}$, $Fe^{III}$ and $Pd^{II}$ metalloligands

In the CSD, to date, there are 59 reported transition metal complexes with bispidine ligands having the pentadentate structure common to **L2** and to the inner site of **L5** (**L4**). Of these, the majority are with $Fe^{II}$ and $Cu^{II}$ ions. This marked predominance can be easily explained as an effect of the sustained interest, over the years, on their properties in terms of catalytic activity in oxidation or aziridation reactions, and in $^{64}Cu^{II}$ imaging.[15,16] Only eight structures were reported with $Mn^{II}$,[20] four with $Fe^{III}$,[20c,21] and none with $Pd^{II}$, which makes complex of **L4** with $Pd^{II}$ a first of this kind.

The X-ray structure of the $Mn^{II}$ complex, of composition [$Mn^{II}$(**L4**)(Cl)]Cl·1,2DCB (Scheme 2a), is shown in Figure 1a; the metal center is found in a distorted octahedral geometry, with

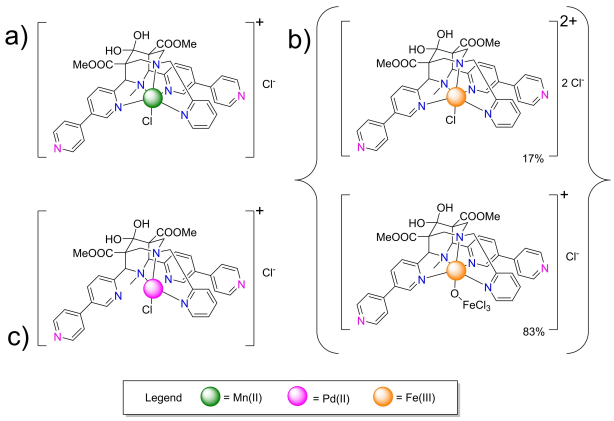


**Scheme 2.** Chemical formulae of metal complexes made with **L4** characterized by SC-XRD: a) {[$Mn^{II}$(**L4**)(Cl)]Cl·1,2-DCB}, b) {[$Fe^{III}$(**L4**)Cl]$Cl_2$ (17%)/[$Fe^{III}$-(**L4**)(Cl)]O-$FeCl_3$ (83%)}, and c) {[$Pd^{II}$(**L4**)(Cl)]Cl·$CHCl_3$·$H_2O$} (Table S2 and S3 in Supporting Information).

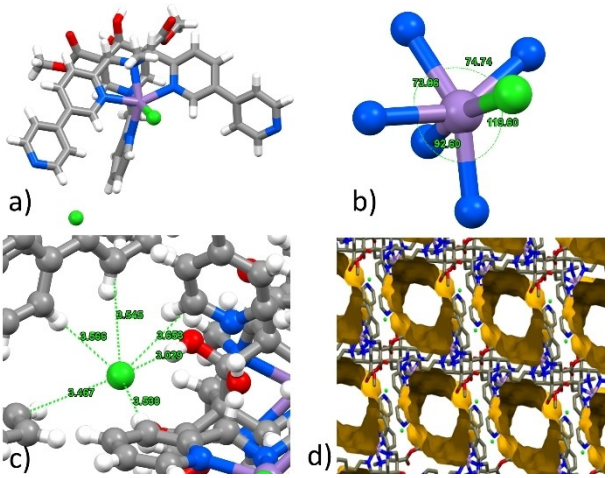


**Figure 1.** a) View of [$Mn^{II}$(**L4**)(Cl)]Cl; b) distorted octahedral coordination geometry of the $Mn^{II}$ ion; c) view of the non-coordinated chloride ion and its interactions with the environment; d) view of the void space generated by virtual removal of the solvent present (it accounts for 29.3% of the total unit cell volume). Color code: C = dark grey; H = white; N = blue; O = red; Cl = green; Mn = light violet.

Research Article
doi.org/10.1002/ejic.202200221



the ligand occupying five sixths of the coordination sphere, completed by a chloride ion (Figure 1b). The packing is directed by two main elements, which are the chloride counterion, and the 1,2-DCB solvent molecules entrapped within the lattice. The former, at 7.643 Å distance from the closest $Mn^{II}$ center, directs the assembly around itself of four complexes (Figure 1c) via several $CH_{arom}\cdots Cl^-$ hydrogen bond (HB) interactions (C···Cl distances in the 3.467–3.653 Å range) with pyridine rings, and *via* one OH···$Cl^-$ HB with the gem-diol unit (O···Cl distance of 3.029 Å), similar to what is observed in other examples of second sphere coordination in polypyridyl metal complexes.[22] The solvent has also an important role in the final structure, adopting two different locations, being disordered in one of them, and displaying no evidence of any strong specific interaction with neither metalloligands nor counteranions. Interestingly, it resides within a channeled framework which, if virtually evacuated, would possess void space corresponding to 29.3% of the total unit cell volume (Figure 1d).

The X-ray structure of the $Fe^{III}$ complex with **L4** (Scheme 2b) is shown in Figure 2a. In this case, within the crystal, two species were found in an approximately 8:2 ratio, disordered over the same crystallographic site. Indeed, the $Fe^{III}$ center coordinated by the ligand **L4** completes its distorted octahedral coordination sphere (Figure 2b) with either a chloride (approx. 17%) or with a $[Fe^{III}OCl_3]^{2-}$ dianion, disordered over two positions (ca. 83% in total) connected by a bridging μ-O atom. This particular μ-oxo-diferric unit has already been reported in several occasions.[23] Centrosymmetrically oriented pairs of [**L4**-$Fe^{III}$-Y] (Y=$Fe^{III}OCl_3$ or Cl) units (Figure 2c), also interacting via evident $CH_{arom}\cdots$Cl–Fe intermolecular contacts, are arranged parallelly to each other and glued together by surrounding chloride counteranions (Figure 2d) which, as in the previous example, display $CH_{arom}\cdots Cl^-$ interactions with at least three different ligands (C···$Cl^-$ distances in the 3.476–3.605 Å range) and one OH···$Cl^-$ HB interaction (O···Cl distance of 3.089 Å) with the gem-diol unit.

The last complex we succeeded to isolate and characterize by SC-XRD is that of **L4** with $Pd^{II}$, of composition [[$Pd^{II}$-(**L4**)(Cl)]Cl·$CHCl_3$·$H_2O$ (Scheme 2c), whose X-ray structure is depicted in Figure 3a. This is the first $Pd^{II}$ complex with a bispidine ligand having a **L2**-like structure. Given the strong preference of the $Pd^{II}$ ion for square planar coordination geometries and the marked difference in the donor character of $N_{aliphatic}$ vs $N_{arom}$, it is not a surprise to find that the pyridine side arms of **L4** are not involved in the metal coordination (Figure 3b). As far as the coordination geometry is concerned, a useful comparison can be made with the cisplatin analogous $Pt^{II}$ and the $Pd^{II}$ complexes reported by Pörschke *et. al.*.[24] This highlights the rigidity of the bispidine core and the small perturbation of the two bipyridyl sidearms of **L4** to the coordination of a metal ion with a square-planar coordination geometry preference satisfied with the inner aliphatic Ns, the appended methyl-pyridyl group and a Cl. Two different solvent molecules, water and chloroform, are found within the lattice, both interacting with the chloride counteranion via CH···$Cl^-$ (3.358 Å) and OH···$Cl^-$ (3.139 Å) HB interactions (Figure 3c). The gem-diol moiety of **L4** ligand is also H-bonded to the chloride, as well as to the water molecule (OH···$Cl^-$ distance of 3.061 Å and OH···$O_w$ distance = 2.686 Å). The water molecule is also interacting with the external divergent pyridine ring N (N···HO distance = 2.845 Å). Chloroform molecules are found aligned in narrow 1D columns made of stretched antiparallel pairs which, if virtually liberated by the solvents, would correspond to ca. 19.6% of the total unit cells (Figure 3d).

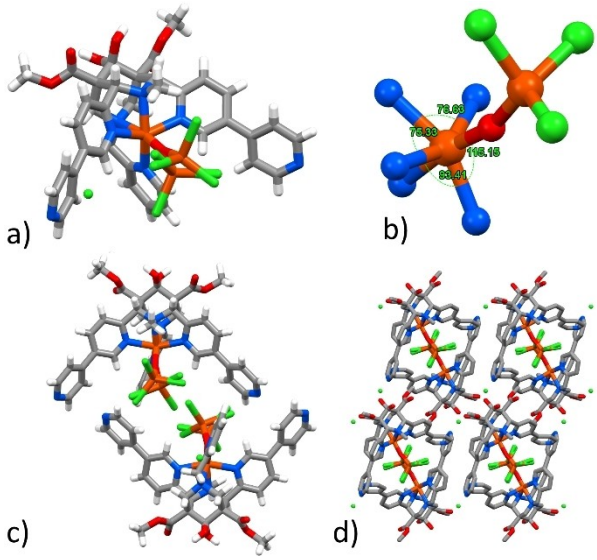


**Figure 2.** a) View of [$Fe^{III}$(**L4**)($Fe^{III}OCl_3$)]Cl (only the major 83% component is shown), and of b) the distorted octahedral coordination geometry of the $Fe^{III}$ ion (for one of the two disordered $OFeCl_3$ moieties); c) view of centrosymmetrically oriented pairs, which are the repeating units in the d) crystal packing. Color code: C = dark grey; H = white; N = blue; O = red; Cl = green; Fe = orange.

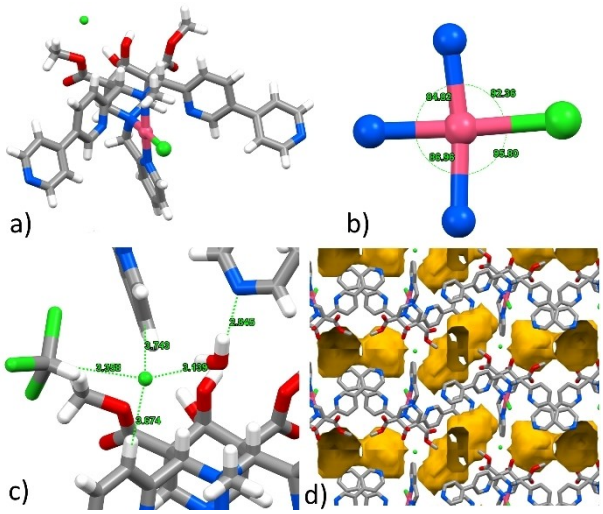


**Figure 3.** a) View of [$Pd^{II}$(**L4**)(Cl)]Cl; b) distorted octahedral coordination geometry of the $Pd^{II}$ ion; c) view of the uncoordinated chloride ion and its interactions with the environment; d) view of the void space, composed of not connected pockets, generated by virtual removal of the solvent present (ca. 19.6% of the total unit cell volume). Color code: C = dark grey; H = white; N = blue; O = red; Cl = green; Pd = purple.

Research Article
doi.org/10.1002/ejic.202200221


All attempts to obtain good quality SCs for $Cu^{II}$ complexes failed so far. Compounds $[Cu^{II}(\mathbf{L4})(Cl)]Cl$ and $[Cu^{II}(\mathbf{L4})(OTf)]OTf$ were obtained as powder microcrystalline materials and were analyzed by ESI-MS and elemental analysis [25] (a partial structural solution from SC data of $[Cu^{II}(\mathbf{L4})(OTf)]OTf$ is in Figure S10a in SI).

## The road to CP: strategy and intermediate species

Metalloligands of composition $[Cu^{II}(\mathbf{L4})(Cl)]Cl$ and $[Cu^{II}(\mathbf{L4})(OTf)]OTf$ were employed as precursors in the second step reaction towards heterometallic CP formation. Based on previous knowledge on CPs formed with **L3**, and similar derivatives,[14] two possible outcomes in terms of topology of the resulting CP could be expected. They are *i*) ribbon like 1D CPs, which feature a 2:1 metalloligand to metal ratio, or *ii*) zig-zag 1D arrays having a 1:1 metalloligand to metal ratio (Scheme 3).[26] Therefore, we set out to a series of crystallization trials employing 2:1 and 1:1 stoichiometric ratios between the metalloligand and the second metal salt species. A list of all attempts made can be found in the Supporting Information (Table S1). Initially, in two occasions, we were able to obtain SCs of heterometallic species, which we attempted to fully characterize.

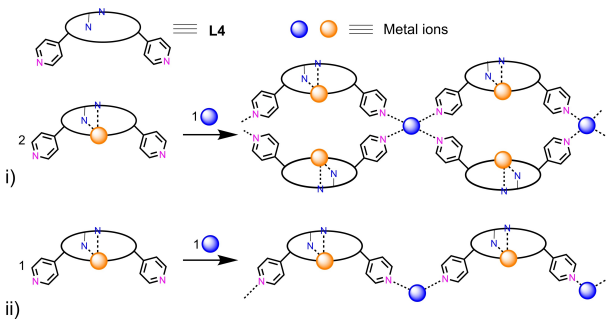


**Scheme 3.** Schematic view of the synthetic strategies leading to i) ribbon-like or ii) zig-zag like coordination polymer topologies.

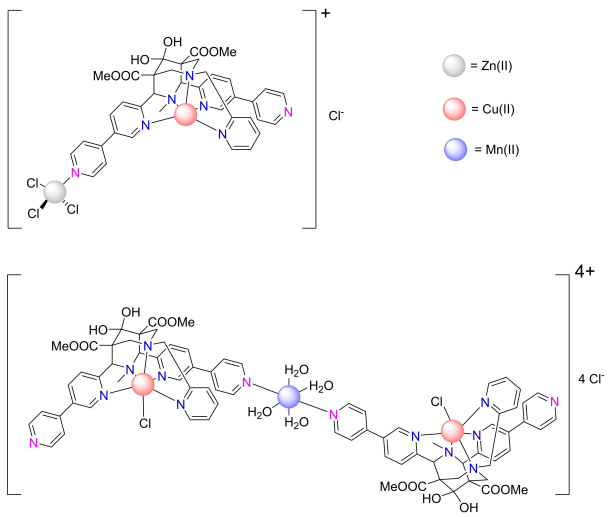


**Scheme 4.** Chemical formulae of metal complexes of **L4**, representing intermediate species along the path from molecular complexes towards CPs; see also Figure 4, below.

They are the molecular complexes described in Scheme 4. As no CPs were isolated, these experiments represented a failure in terms of reaching the proposed CP, but they show possible pitfalls one might experience when heterometallic architectures are sought. Unfortunately, for both structures, we were not able to reach a full and satisfactory SC X-ray data analysis, and a thorough structure solution was thus unattainable; this problem notwithstanding, the basic connectivity can be considered reliable in both cases.

The first heterobimetallic complex was obtained by reacting $[Cu^{II}(\mathbf{L4})(Cl)]Cl$ and $ZnCl_2$ in a 2:1 ratio using a MeCN/1,2-DCB mixture as crystallization solvent (Scheme 4 and Figure 4a). In this case, the internal coordination site provided by **L4** tightly binds a $Cu^{II}$ center, which is found in square pyramidal geometry, while one of the two divergent pyridyl arms of the ligand interacts with a $Zn^{II}$ ion. The latter is in a tetrahedral environment with three coordinated chloride anions. Disorder is present on the ligand and in a 1,2-DCB solvent molecule, trapped in the lattice. By taking the coordinative connectivity into account –(CuZnCl)···(CuZnCl)– linear arrays can be visualized (Figure S10b in Supporting Information).

A second species that deserves to be mentioned here is that obtained by reacting $[Cu^{II}(\mathbf{L4})(OTf)]OTf$ with $MnCl_2$ in MeOH. It shows a trinuclear bis-metalloligand heterometallic complex (Scheme 4 and Figure 4b). The $Cu^{II}$ metal ion displays an octahedral environment, with the initial $OTf^-$ anion replaced by a chloride. One divergent pyridine unit of each of the two

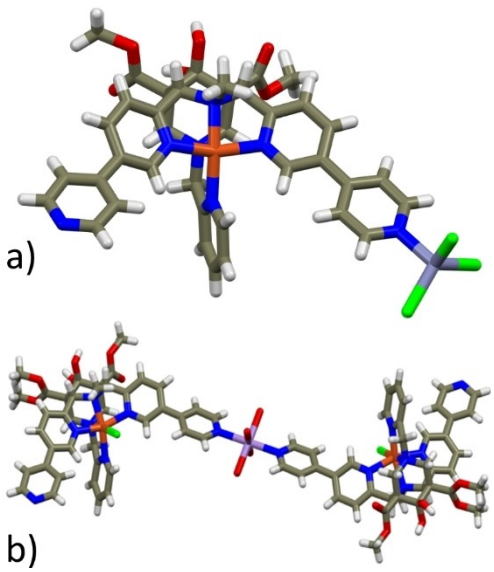


**Figure 4.** View of two heterometallic molecular complexes: a) $[Cu^{II}(\mathbf{L4})(Zn^{II}Cl_3)]Cl$ (Cl counteranion is assumed as it cannot be located by SC-XRD data), and b) $[Cu^{II}(\mathbf{L4})(Cl)]_2[Mn^{II}(H_2O)_4]$. No suitable SC-XRD data were available, thus these representations serve the only purpose of clarifying the metal-ligand connectivity. Color code: C = dark grey; H = white; N = blue; O = red; Cl = green; Zn = purple; Cu = orange; Mn = light violet.

Research Article
doi.org/10.1002/ejic.202200221


metalloligands is bound to a $Mn^{II}$ ion, representing the center of symmetry, saturated by four additional water molecules. On the other side of the ligands, the divergent pyridine N is bound to a water molecule, and this surely contributes to hamper the coordinative polymerization.

### First heterobimetallic bispidine CP

Slow evaporation of a 1:1 mixture of [$Cu^{II}$(**L4**)(OTf)]OTf and $Zn(NO_3)_2$ in MeCN afforded good quality SCs, whose X-ray diffraction characterization revealed to consist in the desired heterobimetallic 1D ribbon-like coordination polymer of composition {[$Cu^{II}$(**L4**)(MeCN)]$_2$(OTf)$_4$-[$Zn^{II}$($H_2O$)$_2$]($NO_3$)$_2$($MeCN$)$_2$($H_2O$)}$_n$. A view of the 1D arrays is pictured in Figure 5a, where counteranions and solvent molecules not coordinated to the metal centers are omitted. The CP resembles the ribbon-like CPs based on **L3** (having shorter arms and no convergent pyridine sites, see Scheme 1b), and this confirms the validity of our design. The coordination of four pyridine units, belonging to four different metalloligand sidearms, to the $Zn^{II}$ ions generates an array composed of repeating 32-membered metallomacrocycles. Both metal ions are in an octahedral environment, partially filled by solvents. The $Zn^{II}$ coordination sphere is completed by two apical water molecules, while **L4** provides the $Cu^{II}$ center with five donor atoms. The sixth position is occupied by a MeCN molecule with a Cu···$NCCH_3$ distance of 2.747 Å (Figure 5b). The metric analysis allows to infer about a quite easily exchangeable MeCN molecule, considering that the Cu···$N_{MeCN}$ distance is the longest among the collection of known structures of a single MeCN molecule coordinated to an octahedral $Cu^{II}$ with the other five donor atoms being Ns (Figure S11 in Supporting Information).[27] Thus, at variance with the previously described metalloligand structures, the three counteranions present in the asymmetric unit, two $OTf^-$ and one $NO_3^-$, derived from the metalloligand and the $Zn^{II}$ salt used in the synthesis, are not found in the first coordination sphere of neither of the two metal ions. They are found instead establishing several different types of interactions with **L4** and with the solvents present (see Figure S12a in Supporting Information). Indeed, two MeCN and a water molecule are also trapped within the framework. This multitude of species provides no possibility for a porous structure, and even a virtual removal of the solvent molecules, which occupy 13.2% of the total unit cell volume, does not generate channels but only not-interconnected pockets (Figure S12b in Supporting Information). This structural aspect might hamper the capability of CP **1** to be active in heterogeneous catalysis, although 1D CPs have shown to be permeable to guest molecules or solvents even when being non-porous.[1d,14] The packing is characterized by linear arrays aligned along the *b*-axis and parallel to each other, offset by about 5 Å. Reproducing the CP **1** SC phase in the form of microcrystalline powders would allow to test the material for catalytic purposes. In Figure 6, the P-XRD pattern (black) of a powder obtained by reacting [$Cu^{II}$-(**L4**)(OTf)]OTf and $Zn(NO_3)_2$ in MeCN at 50 °C for 1 h (Supporting Information) is compared with the simulated P-XRD pattern (red) corresponding to the CP **1** SC phase. The agreement between the two diffractograms is fair, and this result is promising for the production of the CP **1** material in larger scale, suitable for catalytic activity testing.

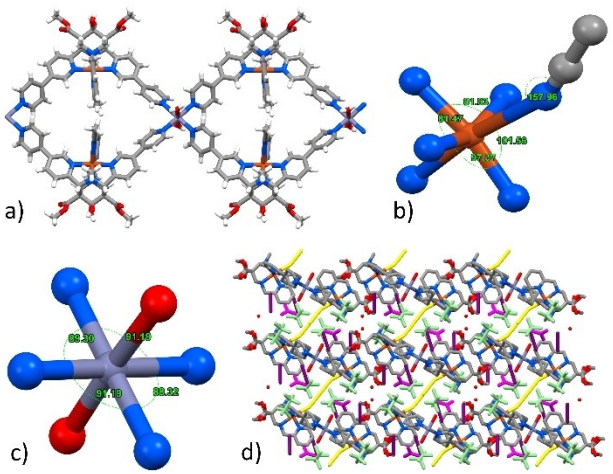


**Figure 5.** a) View of repeating macrocycles constituting the ribbon-like CP arrays of **1**; b) view of the distorted octahedral coordination geometry of $Cu^{II}$ within the inner bisbidine binding site, and c) octahedral coordination geometry of $Zn^{II}$ responsible for the coordinative polymerization; d) view of the packing along the x-axis, evidencing the many different species present, including solvents and counterions (OTf = light green, $NO_3^-$ = violet; MeCN = dark violet; $Cu^{II}$-bound MeCN = yellow). Color code: C = dark grey; H = white; N = blue; O = red; Zn = purple; Cu = orange.

## Conclusion

Heterometallic CPs are a rising class of materials with incredible potential in future applications. On the basis of the synergic exploitation of the combination of two or more metal sites, each one dedicated to a specific function, novel properties and functions may arise. In this work, we aimed at the design of

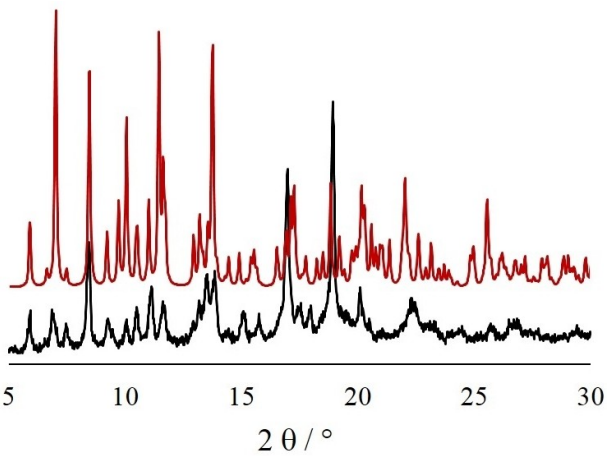


**Figure 6.** Comparison between the P-XRD pattern of the powder sample obtained by reacting $Cu^{II}$(**L4**)(OTf)]OTf with $Zn(NO_3)_2$ in MeCN (black) and the simulated pattern derived from SC data of CP **1**.

Research Article
doi.org/10.1002/ejic.202200221





novel materials that could possess the catalytic activity of well-known bispidine based molecular complexes, such as those derived from **L1** and **L2**, and, in addition, could open the way to heterogeneous process conditions, considered more efficient for large scale, real world applications.[17] The bispidine scaffold, such as in **L3** and its derivatives, has indeed proved to be quite useful in the design of 1D coordination polymers with highly dynamic behavior in terms of guest adsorption and exchange processes.[14] Therefore, in order to introduce additional functionalities and exploit the inner aliphatic Ns, ligand **L5** was designed. It features the classic pentadentate bispidine ligand environment and, at the same time, it is decorated with adjunct divergent pyridine moieties that can lead to coordinative polymerization. We have made use of a classic strategy (*via* metalloligand)[9] to create the first $Cu^{II}/Zn^{II}$ heterobimetallic bispidine CP, **1**, obtained as SC and analyzed in detail by SC-XRD, and reproduced as microcrystalline powder. We have also reported a series of metalloligands with $Mn^{II}$, $Fe^{III}$, $Cu^{II}$ and $Pd^{II}$ metal centers and identified two intermediate species, alas only partially characterized, along the route to CP formation. Although CP **1** might not have all the requirements for being successful in the desired application, its isolation and full characterization indeed supports the quality of our synthetic approach and opens the way to a large variety of heterobimetallic 1D CPs with tunable properties, whose syntheses and testing are currently ongoing in our laboratories.

## Experimental Section

All reagents were of reagent grade and were used as received without further purification. X-ray data were collected at low temperature with an Agilent Technologies Supernova-E CCD diffractometer. NMR spectra were recorded on a Bruker Avance 400 MHz; Powder X-ray diffraction was carried out at room temperature with a Bruker D2-Phaser diffractometer (Cu radiation) using Bragg-Brentano geometry. ESI-MS spectra were acquired on a Bruker Esquire 3000 PLUS instrument with quadrupole ion trap detector. Elemental analysis was performed with a Costech ECS 4010 instrument.

Synthesis of **L5**: Dimethyl-1,3-acetonedicarboxylate (1.3 g, 7.47 mmol) was dissolved in 20 mL of MeOH and then 2 eq. of [3,4′-bipyridine]-6-carbaldehyde[28] (14.9 mmol, 2.75 g) were added. After cooling the mixture at 0 °C using an ice bath methyl amine (1 eq., 0.62 mL, 40% water sol.) was added. The reaction was left under stirring at r.t. for 18 hours. After that time, a white precipitate was formed. It was filtered, washed with cold MeOH and recrystallized from MeOH to afford 3 g of the intermediate piperidone **A** (Supporting Information), which was utilized in the next step without additional purification. Piperidone **A** (2 g, 3.72 mmol) was dissolved in 25 mL of MeOH and a methanolic solution of 6 eq. of formaldehyde ((37% w, 1.66 mL) and 3 eq. of 2-picolyamine (11.2 mmol, 1.2 g) was added. After 9 hours of stirring at 80 °C, the heating was stopped. After cooling at room temperature, a white powder precipitated. This solid was filtered and washed with cold MeOH affording 1.8 g of the desired product **L5** (ca. 72% yield).

**L5**: $^{1}$H-NMR (400 MHz, $CDCl_3$): δ 8.73 (m, 7H), 8.14 (d, $J=8$ Hz, 2H), 7.80 (dd, $J=2.4$ Hz, 2H), 7.70 (td, $J=8.3$ Hz, 1H), 7.48 (dd, $J=4.5$ Hz, $J=1.6$ Hz, 4H), 7.33 (m, 1H), 4.88 (s, 2H), 3.84 (s, 6H), 3.66 (s, 2H), 3.23 (d, $J=12.2$ Hz, 2H), 2.80 (d, $J=12.2$ Hz, 2H), 2.06 (s, 3H), ppm;$^{13}$C-NMR (100 MHz, DMSO-$d_6$): 203.9, 168.4, 159.2, 157.2, 149.7, 147.5, 144.2, 137.3, 135.3, 132.3, 125.2, 124, 123.2, 121.7, 73.2, 62.9, 62.3, 59.2, 52.8, 43.3 ppm. ESI-MS: m/z calcd. for $C_{38}H_{35}N_7O_5$ 669.27 found 670.2 $[M+H]^+$, 692.6 $[M+Na]^+$; 702.6 $[M+H+MeOH]^+$

$[Cu^{II}(\mathbf{L4})(OTf)]OTf$: **L5** (400 mg, 0.6 mmol,) and $Cu(OTf)_2$ (217 mg, 0.6 mmol) were dissolved in dry $CH_3CN$ (10 mL). The reaction was refluxed and left under stirring in inert conditions for 24 hours. After cooling at room temperature, a blue precipitate was formed. It was filtered and washed with cold MeOH to afford $[Cu^{II}(\mathbf{L4})(OTf)]OTf$ (535 mg, 85%).[25] ESI-MS (MeOH): calcd. for $C_{39}H_{35}CuF_3N_7O_8S^+$ 881.15, found: 881.2 $[Cu^{II}(\mathbf{L5})(OTf)]^+$, 899.2 $[Cu^{II}(\mathbf{L4})(OTf)]^+$ or $\{[Cu^{II}(\mathbf{L5})(OTf)]+H_2O\}^+$; 913.2 $\{[Cu^{II}(\mathbf{L5})(OTf)]+MeOH\}^+$. Elem. Anal. C, 45.78; H, 3.55; N, 9.34; calcd. for $C_{40}H_{37}CuF_6N_7O_{12}S_2$, found: C, 44.84; H, 3.94; N, 8.92.

$[Cu^{II}(\mathbf{L4})(Cl)]Cl$: **L5** (360 mg, 0.48 mmol) and $CuCl_2$ (0.48 mmol, 64.53 mg) were dissolved in dry $CH_3CN$ (10 mL). The reaction was refluxed and left under stirring under inert conditions for 24. After cooling to r.t., a blue precipitate was obtained, which was then filtered and washed with cold methanol to afford338 mg of $[Cu^{II}(\mathbf{L4})(Cl)]Cl$ (yield 88%).[25]

ESI-MS (MeOH): m/z calcd. for $C_{38}H_{37}CuClN_7O_6^+$ 785.2, found 785.3 $[Cu^{II}(\mathbf{L4})(Cl)]^+$ or $\{[Cu^{II}(\mathbf{L5})(Cl)]+H_2O\}^+$, 799.2 $\{[Cu^{II}(\mathbf{L5})(Cl)]+MeOH\}^+$, 863.3 $[Cu^{II}\mathbf{L5}(Cl)(MeOH)_3]$, 877.3 $[Cu^{II}(\mathbf{L4})(Cl)_2+H_2O+K]^+$. Elem. Anal.: C, 54.32; H, 4.68; N, 11.67; calcd. for $C_{38}H_{35}Cl_2CuN_7O_5+H_2O$, found: 54.88; H, 4.90; N, 11.92.

2128217 (for **L5**·MeCN), 2128218 (for [**L4**-$Fe^{III}$-Y] (Y = $Fe^{III}OCl_3$ or Cl)), 2128219 (for $[Mn^{II}(\mathbf{L4})(Cl)]Cl$), 2128220 (for $[Pd^{II}(\mathbf{L4})(Cl)]Cl$), and 2128221 (for CP **1**)

Deposition Numbers 2128217 (for **L5**·MeCN), 2128218 (for [**L4**-$Fe^{III}$-Y] (Y=$Fe^{III}OCl_3$ or Cl)), 2128219 (for $[Mn^{II}(\mathbf{L4})(Cl)]Cl$), 2128220 (for $[Pd^{II}(\mathbf{L4})(Cl)]Cl$), and 2128221 (for CP **1**) contain the supplementary crystallographic data for this paper. These data are provided free of charge by the joint Cambridge Crystallographic Data Centre and Fachinformationszentrum Karlsruhe Access Structures service www.ccdc.cam.ac.uk/structures.

## *Acknowledgements*

*M.C. acknowledges Fondo per il finanziamento delle attività base di ricerca FFABR-MIUR. Heidelberg University is gratefully acknowledged for financial support. Open Access Funding provided by Politecnico di Milano within the CRUI-CARE Agreement.*

## *Conflict of Interest*

The authors declare no conflict of interest.

## Data Availability Statement

The data that support the findings of this study are available from the corresponding author upon reasonable request.

**Keywords:** Coordination polymers · Heterometallic · Metalloligand approach · Transition metal complexes · X-ray structures

[1] a) S. R. Batten, S. M. Neville, D. R. Turner, *Coordination Polymers Design, Analysis and Application*, *The Chemistry of Metal-Organic Frameworks Synthesis*, *Characterization and Applications*, S. Kaskel (Ed.), Wiley-VCH Verlag GmbH & Co, Weinheim, Germany **2016**; b) H. Furukawa, K. E. Cordova, M. O'Keeffe, O. M. Yaghi, *Science* **2013**, *341*, 974; c) S. L. Griffin, N. R. Champness, *Coord. Chem. Rev.* **2020**, *414*, 213295; d) M. Lippi, M. Cametti, *Coord. Chem. Rev.* **2021**, *430*, 213661; e) S. Hasegawa, S. Horike, R. Matsuda, S. Furukawa, K. Mochizuki, Y. Kinoshita, S. Kitagawa, *J. Am. Chem. Soc.* **2007**, *129*, 9, 2607–2614; f) D. Sheberla, L. Sun, M. A. Blood-Forsythe, S. Er, C. R. Wade, C. K. Brozek, A. Aspuru-Guzik, M. Dincă, *J. Am. Chem. Soc.* **2014**, *136*, 25, 8859–8862.

[2] a) W. L. Leong, J. J. Vittal, *Chem. Rev.* **2021**, *111*, 688–764; b) L.-P. Tang, S. Yang, D. Liu, C. Wang, Y. Ge, L.-M. Tang, R.-L. Zhou, H. Zhang, *J. Mater. Chem. A* **2020**, *8*, 14356.

[3] A. Kumar Ghosh, A. Hazra, A. Mondal, P. Banerjee, *Inorg. Chim. Acta* **2019**, *488*, 86–119; J.-M. Lehn, in *Supramolecular Chemistry: Concepts and Perspectives*, Wiley-VCH **1995**.

[4] S. M. Moosavi, A. Nandy, K. M. Jablonka, D. Ongari, J. P. Janet, P. G. Boyd, Y. Lee, B. Smit, H. J. Kulik, *Nat. Commun.* **2020**, *11*, 4068.

[5] T.-H. Chen, I. Popov, W. Kaveevivitchai, O. Š. Miljanić, *Chem. Mater.* **2014**, *26*, 4322.

[6] a) M. K. Bera, Y. Ninomiya, M. Higuchi, *Commun. Chem.* **2021**, *4*, 56; b) J. Li, Y. Tan, C. Cao, Z.-K. Wang, Z. Niu, Y.-L. Song, J.-P. Lang, *CrystEngComm* **2021**, *23*, 3160; c) Q. Xu, Z. Chen, H. Min, F. Song, Y.-X. Wang, W. Shi, P. Cheng, *Inorg. Chem.* **2020**, *59*, 6729–6735; d) F. Moutier, A. M. Khalil, S. A. Baudron, C. Lescop, *Chem. Commun.* **2020**, *56*, 10501; e) A. C. M. San Esteban, N. Kuwamura, N. Yoshinari, T. Konno, *Dalton Trans.* **2021**, *50*, 14730–14737; f) A. Bhunia, M. A. Gotthardt, M. Yadav, M. T. Gamer, A. Eichhçfer, W. Kleist, P. W. Roesky *Chem. Eur. J.* **2013**, *19*, 1986–1995.

[7] a) Ü. Kökçam-Demir, A. Goldman, L. Esrafili, M. Gharib, A. Morsali, O. Weingart, C. Janiak, *Chem. Soc. Rev.* **2020**, *49*, 2751–2798; b) L. Jiewei, C. Lianfen, C. Hao, Z. Jianyong, Z. Li, S. Cheng-Yong, *Chem. Soc. Rev.* **2014**, *43*, 6011–6061; c) L. J. Murray, M. Dincă, J. Yano, S. Chavan, S. Bordiga, C. M. Brown, J. R. Long, *J. Am. Chem. Soc.* **2010**, *132*, 7856–7857; d) H. K. Kim, W. S. Yun, M.-B. Kim, J. Y. Kim, Y.-S. Bae, J. Lee, N. C. Jeong, *J. Am. Chem. Soc.* **2015**, *137*, 31, 10009–10015; e) G. Akiyama, R. Matsuda, H. Sato, S. Kitagawa, *Chem. Asian J.* **2014**, *9*, 2772–2777.

[8] a) A. J. Lewis, E. Garlatti, F. Cugini, M. Solzi, M. Zeller, S. Carretta, C. M. Zaleski, *Inorg. Chem.* **2020**, *59*, 17, 11894–11900; b) A. Chakraborty, J. Goura, P. Kalita, A. Swain, G. Rajaraman, V. Chandrasekhar, *Dalton Trans.* **2018**,*47*, 8841–8864.

[9] a) G. Kumar, R. Gupta, *Chem. Soc. Rev.* **2013**, *42*, 9403; b) J.-R. Li, D. J. Timmons, H.-C. Zhou, *J. Am. Chem. Soc.* **2009**, *131*, 6368–6369; c) P. Liebing, F. Oehler, J. Witzorke, M. Schmeide, *CrystEngComm* **2020**, *22*, 7838; d) X.-Z. Li, P.-P. Hao, D. Wang, W.-Q. Zhang, L.-N. Zhu, *CrystEngComm* **2012**,*14*, 366–369.

[10] N. Kuwamura, T. Konno, *Inorg. Chem. Front.* **2021**, *8*, 2634.

[11] P. Comba, M. Kerscher, W. Schiek, *Bispidine Coordination Chemistry, Progress in Inorganic Chemistry*, **2005**, vol. 55, Chapter 9, 613.

[12] a) P. Comba, C. Lopez de Laorden, H. Pritzkow, *Helv. Chim. Acta* **2005**,*88*, 647; b) P. Comba, M. Kerscher, K. Rück, M. Starke, *Dalton Trans.* **2018**, *47*, 9202–9220.

[13] a) L. Abad-Galàn, P. Cieslik, P. Comba, M. Gast, O. Maury, L. Neupert, A. Roux, H. Wadepohl, *Chem. Eur. J.* **2021**, *27*, 10303–10312; b) P. Cieslik, P. Comba, W. Hergett, R. Klingeler, G. F. P. Plny, L. Spilleke, G. Z. Velmurugan, *Anorg. Allg. Chem.* **2021**, *647*, 843–849.

[14] a) M. Lippi, J. Caputo, A. Famulari, C. Castellano, F. Meneghetti, J. Marti-Rujas, M. Cametti, *Dalton Trans.* **2020**, *49*, 13420–13429; b) M. Lippi, J. Caputo, A. Famulari, A. Sacchetti, C. Castellano, F. Meneghetti, J. Marti-Rujas, M. Cametti, *Dalton Trans.* **2019**, *49*, 5965–5973; c) M. Lippi, M. Cametti, J. Marti-Rujas, *Dalton Trans.* **2019**, *48*, 16756–16763; d) A. Rossetti, M. Lippi, J. Marti-Rujas, A. Sacchetti, M. Cametti, *Chem. Eur. J.* **2018**, 24,19368–19372.

[15] a) P. Comba, C. Lang, C. Lopez de Laorden, A. Murugantantham, G. Rajaraman, H. Wadepohl, M. Zajaczkowski, *Chem. Eur. J.* **2008**, *14*, 5313–5328; b) P. Comba, Y.-M. Lee, W. Namb, A. Waleska, *Chem. Commun.* **2014**, *50*, 412–414; c) P. Comba, M. Merz, H. Pritzkow, *Eur. J. Inorg. Chem.* **2003**, 1711; d) P. Comba, B. Martin, A. Muruganantham, J. Straub, *Inorg. Chem.* **2012**, *51*, 9214–9225; e) P. Comba, G. Rajaraman, *Inorg. Chem.* **2008**, *47*, 78; f) P. Comba, S. Wunderlich, *Chem. Eur. J.* **2010**, *16*, 7293–7299; g) P. Comba, S. Fukuzumi, C. Koke, A. M. Löhr, J. Straub, *Angew. Chem. Int. Ed.* **2016**, *55*, 11129–11133; *Angew. Chem.* **2016**, *128*, 11295–11299; h) F. Althoff, K. Benzing, P. Comba, C. McRoberts, D. R. Boyd, S. Greiner, F. Keppler, *Nat. Commun.* **2014**, *5*, 4205.

[16] a) S. Juran, M. Walther, H. Stephan, R. Bergmann, J. Steinbach, W. Kraus, F. Emmerling, P. Comba, *Bioconjugate Chem.* **2009**, *20*, 347–359; b) P. Comba, M. Morgen, H. Wadepohl, *Inorg. Chem.* **2013**, *52*, 6481–6501; c) P. Comba, U. Jermilova, C. Orvig, B. O. Patrick, C. F. Ramogida, K. Rück, C. Schneider, M. Starke, *Chem. Eur. J.* **2017**, *23*, 15945–15956; d) G. Singh, K. Zarschler, S. Hunoldt, I. I. Santana Martinez, C. Rühl, M. Matterna, R. Bergmann, D. Mathe, N. Hegedüs, M. Bachmann, P. Comba, H. Stephan, *Chem. Eur. J.* **2020**, *26*, 1989–2001.

[17] a) X. Cui, W. Li, P. Ryabchuk, K. Junge, M. Beller, *Nat. Catal.* **2018**, *1*, 385–397; b) R. A. van Santen, in *Modern Heterogeneous Catalysis – An Introduction*, Wiley VCH, Weinheim, Germany **2017**.

[18] J. M. Rujas, S. Bonafede, D. Tushi, M. Cametti *Chem. Commun.* **2015**, *51*, 12357–12360.

[19] a) P. Comba, A. Hauser, M. Kerscher, H. Pritzkow, *Angew. Chem. Int. Ed.* **2003**, *42*, 4536; b) P. Comba, M. Kerscher, M. Merz, V. Müller, H. Pritzkow, R. Remenyi, W. Schiek, Y. Xiong, *Chem. Eur. J.* **2020**, *8*, 5750.

[20] a) P. Cieslik, P. Comba, D. Ndiaye, E. Toth, G. Velmurugan, H. Wadepohl, *Angew. Chem. Int. Ed.* **2022**, e202115580; b) P. Barman, A. K. Vardhaman, B. Martin, S. J. Worner, C. V. Sastri, P. Comba, *Angew. Chem. Int. Ed.* **2015**, *54*, 2095; c) P. Comba, H. Rudolf, H. Wadepohl, *Dalton Trans.* **2015**, *44*, 2724; d) M. Atanasov, C. Busche, P. Comba, F. El Hallak, B. Martin, G. Rajaraman, J. van Slageren, H. Wadepohl, *Inorg. Chem.* **2008**, *47*, 8112; e) P. Comba, B. Kanellakopulos, C. Katsichtis, A. Lienke, H. Pritzkow, F. Rominger, *J. Chem. Soc. Dalton Trans.* **1998**, 3997–4002.

[21] a) M. Abu-Odeh, K. Bleher, N. J. Britto, P. Comba, M. Gast, M. Jaccob, M. Kerscher, S. Krieg, M. Kurth, *Chem. Eur. J.* **2021**, *27*, 11377–11390; b) P. Comba, H. Wadepohl, A. Waleska, *Aust. J. Chem.* **2014**, *67*, 398–404.

[22] R. Tatikonda, M. Cametti, E. Kalenius, A. Famulari, K. Rissanen, M. Haukka, *Eur. J. Inorg. Chem.* **2019**, 4463–4470.

[23] a) A. Machkour, D. Mandon, M. Lachkar, R. Welter, *Inorg. Chem.* **2004**, *43*, 1545–1550; b) L. Guo, Y. Liu, K. Lian, W. Sun, H. Zhu, Q. Du, Z. Liu, X. Chen, S. Dai, *Eur. J. Inorg. Chem.* **2018**, 4887–4892; c) Y. Yang, C. Lu, H. Wang, X. Liu, *Dalton Trans.* **2016**, *45*, 10289–10296.

[24] a) H. Cui, R. Goddard, K.-R. Pörschke, A. Hamacher, M. U. Kassack, *Inorg. Chem.* **2016**, *55*, 2986; b) H. Cui, R. Goddard, K.-R. Pörschke, *Organometallics* **2011**, *30*, 6241.

[25] ESI-MS data points to the presence of both **L4** and **L5** ligands, while the elemental analysis is obviously not helpful in this respect. We note that the process of addition of water to the carbonyl of **L5**-based complexes to form **L4** complexes is quite effective under crystallization conditions, but it is also reversible. We have $^1$H-NMR evidence, not shown here, that thermal treatment at 100 °C of a $Zn^{II}$ complex analogous to [$Cu^{II}$(**L4**)(Cl)]Cl transforms it into the **L5** derivative [ $Zn^{II}$(**L5**)(Cl)]Cl.

[26] M. Lippi, A. Murelli, P. Rossi, P. Paoli, M. Cametti, *Chem. Eur. J.* **2022**, DOI: 10.1002/chem.202200420.

[27] Also, a fair correlation between $Cu^{II}$–$NCCH_3$ distances and $Cu^{II}$–N–$CCH_3$ angles is found in a series of structurally relevant $Cu^{II}$ complexes (see Figure S11 in Supporting Information).

[28] Y. Yang, J.-H. Jia, X.-L. Pei, H. Zheng, Z.-A. Nan, Q.-M. Wang, *Chem. Commun.* **2015**, *51*, 3804–3807.

Manuscript received: April 8, 2022
Accepted manuscript online: April 12, 2022